FEBS 24715 FEBS Letters 493 (2001) 95–100

A deteriorated triple-helical scaffold accelerates formation of the *Tetrahymena* ribozyme active structure

Yasushi Ohki, Yoshiya Ikawa, Hideaki Shiraishi, Tan Inoue*

Graduate School of Biostudies, Kyoto University, Kyoto 606-8502, Japan

Received 8 January 2001; revised 27 February 2001; accepted 28 February 2001

First published online 13 March 2001

Edited by Judit Ovádi

Abstract The *Tetrahymena* group I ribozyme requires a hierarchical folding process to form its correct three-dimensional structure. Ribozyme activity depends on the catalytic core consisting of two domains, P4–P6 and P3–P7, connected by a triple-helical scaffold. The folding proceeds in the following order: (i) fast folding of the P4–P6 domain, (ii) slow folding of the P3–P7 domain, and (iii) structure rearrangement to form the active ribozyme structure. The third step is believed to directly determine the conformation of the active catalytic domain, but as yet the precise mechanisms remain to be elucidated. To investigate the folding kinetics of this step, we analyzed mutant ribozymes having base substitution(s) in the triple-helical scaffold and found that disruption of the scaffold at A105G results in modest slowing of the P3–P7 folding (1.9-fold) and acceleration of step (iii) by 5.9-fold. These results suggest that disruption or destabilization of the scaffold is a normal component in the formation process of the active structure of the wild type ribozyme.

Key words: Group I intron; Ribozyme; RNA folding; Self-splicing; *Tetrahymena*

1. Introduction

The *Tetrahymena* group I ribozyme that has served as one of the most useful model RNAs for investigation of the RNA folding process forms a complex three-dimensional (3D) structure (Fig. 1A) [1–4]. This ribozyme conducts a self-splicing reaction consisting of two conserved structural domains, P4–P6 and P3–P7, which are connected covalently by two single stranded regions, J3/4 and J6/7 [5,6]. The two domains are packed together to form a conserved core that serves as an active site to stabilize transitional states of chemical reactions [5,7].

To correctly form its complex 3D structure, a hierarchical procedure is followed by the *Tetrahymena* ribozyme (Fig. 1B) [8]. A series of analyses by Zarrinkar and Williamson, and Sclavi et al. determined the rate constants for the formation of the two conserved domains, P4–P6 and P3–P7 (and other regions), and established a basic framework for kinetic folding of the two domains (Fig. 1B) [2,9,10]. In this process, the intermediate secondary structure of the P4–P6 domain (termed I_1) forms rapidly, followed by formation of its tertiary structure (the next intermediate, I_2). I_2 is then converted by the formation of two sets of base triples, J3/4×P6 and J6/7×P4 to result in I_3, which in turn conducts the folding of the P3–P7 domain to form I_F. The conversion from I_2 to I_F mediated by I_3 is distinctively slower than the P4–P6 formation. In the final step, conformational rearrangement of I_F occurs to form the catalytically active structure [2,10].

The overall rate of the folding pathway of the *Tetrahymena* ribozyme ($k_{overall}$) has been shown to depend on the concentration of magnesium ions [11,12]. The rate is optimal at 2 mM Mg^{2+} and decreases gradually with an increase of magnesium ion concentration although the overall framework of folding hierarchy is maintained. Consequently, at 10 mM Mg^{2+} which is often used as the standard for assaying both the folding and the reactions, $k_{overall}$ is approximately 20-fold slower than that at 2 mM Mg^{2+} [12]. Two slow steps are observed in this folding (Fig. 1B): the first is the conversion from I_2 to I_F mediated by I_3; this step corresponds to the folding of the P3–P7 domain. The second is the structural rearrangement from I_F to the active structure (20-fold slower than the first step) [12,13]. It has been shown that the rate of P3–P7 folding (k_{P3-P7}) is only weakly influenced by magnesium ion concentrations ([12] and this study). The reduced $k_{overall}$ at 10 mM Mg^{2+} is mainly attributed to the reduced rate of the structural rearrangement at the last step [12]. However, the mechanism of this important structural rearrangement implicated in direct determination of the active catalytic core conformation remains poorly understood.

To analyze the structural elements in the catalytic core, we have examined the activity of mutant group I ribozymes lacking some of these elements. We found that ribozymes lacking both base triples and the P4–P6 domain are still active, establishing that the P3–P7 domain constitutes the minimal catalytic domain [14]. This result suggests that the base triples enhance the folding and/or reaction of the ribozymes by improving their correct folding and/or stabilizing the active structure of the P3–P7 catalytic domain. We tested this hypothesis by examining the structural rearrangement from I_F to the active structure of the *Tetrahymena* ribozyme.

2. Materials and methods

2.1. Preparation of RNAs

Plasmids encoding mutant ribozymes employed in this study were prepared from the pTZIVSU plasmid [15] using polymerase chain reaction (PCR)-dependent site-directed mutagenesis as described [16], and the constructs verified by DNA sequencing. The template DNAs for in vitro transcription of L-21 *Sca*I forms of the *Tetrahymena* ribozyme and its mutants were generated by 20 cycles of PCR

*Corresponding author. Fax: (81)-75-753 3996.
E-mail: tan@kuchem.kyoto-u.ac.jp

0014-5793/01/$20.00
PII: S0014-5793(01)02279-7

(94°C, 30 s/55°C, 2 s/74°C, 1 min) using KOD DNA polymerase (Toyobo, Japan). For PCR, 1 ng of template plasmid (an appropriate derivative of pTZIVSU) and the following set of primers were used: 5′-TAA-TAC-GAC-TCA-CTA-TAG-GGC-GTC-AAA-TTG-CGG-GAA-AGG-3′ (the promoter sequence for T7 RNA polymerase is underlined) and 5′-ACT-CCA-AAA-CTA-ATC-AAT-AT-3′. In vitro transcription reactions with T7 RNA polymerase were performed as described [17].

2.2. Gain of activity assay and kinetic oligonucleotide hybridization assay

A gain of activity assay for measurement of $k_{overall}$ in the presence of 10 mM Mg^{2+} ions was performed as described by Zarrinkar and Williamson [9]. The final concentrations of L-21 *Sca*I ribozyme and substrate RNA whose 5′ terminus was labeled with ^{32}P (5′-CCCU-CUAAAAA-3′) were 7 and 16 nM, respectively. Cleavage reactions were performed for 30 s. Procedures for the gain of activity assay and kinetic oligonucleotide hybridization assay at 2 mM Mg^{2+} were identical to those at 10 mM Mg^{2+} except that the final concentration of magnesium ions in the folding buffer was reduced to 2 mM.

A kinetic oligonucleotide hybridization assay in the presence of 10 mM Mg^{2+} ions was performed as described by Zarrinkar and Williamson [9,18]. To measure the folding kinetics of the P3–P7 domain, a uniformly ^{32}P-labeled L-21 *Sca*I ribozyme (1 nM) and an oligonucleotide probe complementary to the P3 region (positions A270–G279, 20 μM) were used as described [9,19]. The kinetic oligonucleotide hybridization assay at 2 mM Mg^{2+} was identical to that at 10 mM Mg^{2+} except that the final concentration of magnesium ions in the folding buffer was reduced to 2 mM.

All assays in this study were repeated three times. Experimental errors represent the standard deviation from three independent experiments.

3. Results and discussion

3.1. Design of mutants and experiments

The group I ribozyme possesses two sets of conserved base triples, J3/4×P6 and J6/7×P4, at the interface between P4–P6 and P3–P7 domains (Fig. 1A) [5]. These two sets have been considered to form consecutive base triples constituting a triple-helical scaffold in the ribozyme tertiary structure [6]. J3/4 has been proposed to form base triples by interacting with ribose-2′ OH in the minor groove of P6 [20] whereas J6/7 was shown to form base triples by interactions with base moieties in the major groove of P4 [21]. It is unclear whether J3/4×P6 and/or J6/7×P4 plays any particular role in the folding process.

To examine whether J3/4×P6 and J6/7×P4 act as a combined unit or play independent roles in the folding process, we compared the kinetic folding of two mutant ribozymes, A105G and C260G, which have a base substitution in each of the respective base triples. The A105G mutation is expected to disrupt or destabilize base triples formed by J3/4 and P6 as nuclear magnetic resonance studies of model RNA showed that A105 forms base triples with the C216–G257 base pair in P6 by using the N1 position of A105 and 2′OH of G257 (Fig. 1A) [20]. The C260G mutant was prepared originally by Zarrinkar and Williamson to disrupt or destabilize the J6/7×P4 base triples (Fig. 1A) [10].

In the wild type *Tetrahymena* ribozyme, the structural rearrangement from I_F to the active structure occurs rapidly at 2 mM Mg^{2+}. However, this rapid rearrangement poses difficulties for analysis of the rearrangement step because it is kinetically indistinguishable from the preceding step (P3–P7 folding) [12]. To overcome this technical problem, we investigated the step at 10 mM Mg^{2+} where the kinetic constant can be distinguished without affecting the overall framework of the folding hierarchy (Fig. 1B).

3.2. Folding kinetics of a A105G mutant with a defect in J3/4×P6 at 2 mM Mg^{2+}

To study the folding kinetics and thermodynamic stability of an A105G mutant with defective J3/4×P6 interaction, we determined its folding rate in the presence of 2 mM Mg^{2+}, a concentration that is optimum for the wild type *Tetrahymena* ribozyme (Fig. 2A) [12]. By employing a gain of activity assay that monitors the rate of active ribozyme formation as the magnitude of the first turnover in an RNA cleavage reaction [9], the rate ($k_{overall}$) was measured by varying the folding period in the presence of 2 mM Mg^{2+} where derivatives of the *Tetrahymena* ribozyme are often inactive (Fig. 2A) ([10] and this study). The A105G mutant was found to be active but its $k_{overall}$ (0.68 ± 0.04 min^{-1}) was 1.4-fold slower compared to the wild type (0.94 ± 0.04 min^{-1}).

The rate of P3–P7 folding (k_{P3-P7}) that corresponds to the I_2 to I_F conversion rate was determined by employing a kinetic oligonucleotide hybridization assay that monitors folding of a specific region in self-folding RNAs by using an oligonucleotide complementary to the region [9,19]. The extent of RNA folding is estimated from the accessibility of the oligonucleotide to the specific region. By employing the assay, P3–P7 can be defined as folded when the P3 helix becomes inaccessible to its complementary oligonucleotide (Fig. 2B) [32]. At 2 mM Mg^{2+}, k_{P3-P7} of the A105G mutant (0.77 ± 0.08 min^{-1}) was 1.9-fold slower compared with the wild type (1.5 ± 0.1 min^{-1}). However, k_{P3-P7} of the mutant at 2 mM Mg^{2+} was similar to its $k_{overall}$ (0.68 ± 0.04 min^{-1}) at 2 mM Mg^{2+}. This result suggested that the folding of the P3–P7 domain is the rate limiting step in the formation of an active A105G ribozyme at 2 mM Mg^{2+} as this is consistent with the situation in the wild type ribozyme at 2 mM Mg^{2+} where $k_{overall}$ (0.94 ± 0.04 min^{-1}) is also close to k_{P3-P7} (1.5 ± 0.01 min^{-1}) (Fig. 2A,B) [12].

Table 1

Folding rate	[Mg^{2+}] (mM)	Wild type	A105G	C260G	A105G/C260G
$k_{overall}$	2	0.94 (1.1[b])	0.68	–[a]	–[a]
k_{P3-P7}	2	1.5 (1.2[b])	0.77	–[a]	–[a]
$k_{overall}$	10	0.07 (0.06[b])	0.41	0.06	0.15
k_{P3-P7}	10	1.6 (1.2[b,c], 0.72[d])	0.84	(0.15[d])	0.32

[a]The ribozyme is inactive and its P3–P7 cannot fold stably.
[b]Data from [12].
[c]Data from [23].
[d]Data from [10].

3.3. Folding kinetics of A105G mutant at 10 mM Mg^{2+}

In the presence of 10 mM Mg^{2+}, the rate of folding of the wild type ribozyme is slowed presumably because the intermediate form(s) is stabilized by Mg^{2+} ions [11,12]. At 10 mM Mg^{2+}, the rate limiting step of the kinetics is the conformational change from P3–P7 folding to the active ribozyme (Fig. 1B): the formation of the active ribozyme ($k_{overall}$) is approximately 20-fold slower than that of the P3–P7 domain (k_{P3-P7}) [12].

We compared the folding kinetics of the A105G mutant with the wild type ribozyme at 10 mM Mg^{2+} and found that the active mutant ribozyme is formed 5.9-fold (0.41 ± 0.02 min^{-1}) faster than the active wild type (0.07 ± 0.00 min^{-1}) (Fig. 2A). The efficiency of the mutant ribozyme in cleaving the substrate RNA was maximized (0.61 nM/30 s) after 20 min folding at 10 mM Mg^{2+} (Fig. 2A). The maximal efficiency of the mutant ribozyme in cleaving substrate RNA (0.61 nM/30 s) was nearly identical to that of the wild type folded at 2 mM Mg^{2+} (0.63 nM/30 s), suggesting that most of the population of A105G ribozyme folded into the fully active form within 20 min. The result is quite different from that of the wild type folded at 10 mM Mg^{2+} where only 80% of the ribozyme population is active even after 120 min folding [12].

The $k_{overall}$ of the mutant was only modestly influenced by

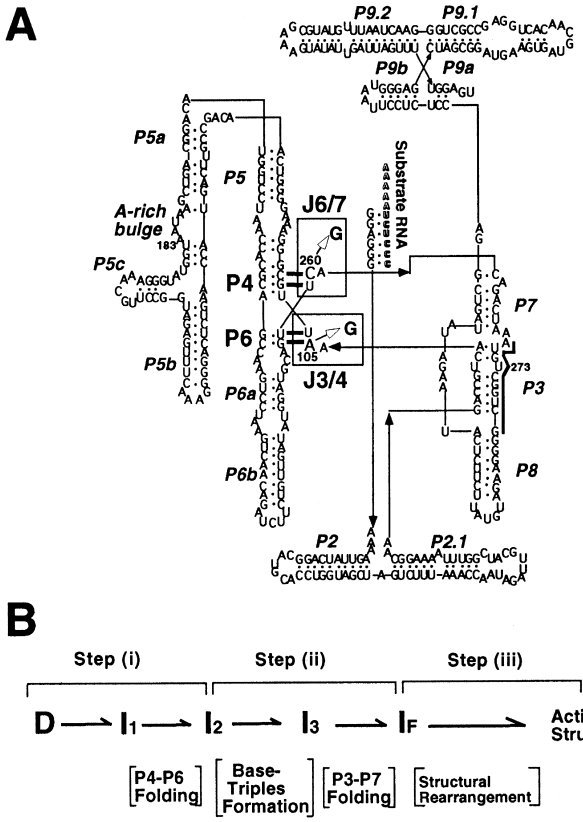

Fig. 1. Structure and folding pathway of the *Tetrahymena* ribozyme. A: The secondary structure of the L-21 *Tetrahymena* ribozyme. The secondary structure of the *Tetrahymena* intron ribozyme is redrawn from [6,31]. Arrowheads superimposed on lines indicate 5′-to-3′ polarity. The P3 sequence targeted by a complementary oligonucleotide probe for kinetic oligonucleotide hybridization assay is indicated with a bold line [9]. The substrate RNA for gain of activity assay is indicated as outline. Mutations analyzed in this study are indicated by white arrows; J3/4 mutant: A105G, J6/7 mutant: C260G, double mutant: A105G/C260G. Positions A183 (A-rich bulge) and U273 (P3 region) that are discussed in the text are also indicated. B: Simplified scheme of the folding pathway of the core region of the L-21 *Tetrahymena* ribozyme. I_1 and I_2 represent the folding intermediates in which the P4–P6 domain forms secondary and tertiary structures, respectively [9]. I_3 represents the intermediate in which the P4–P6 domain and four consecutive base triples are formed [10]. I_F represents the intermediate in which both P4–P6 and P3–P7 domains are folded [4,10].

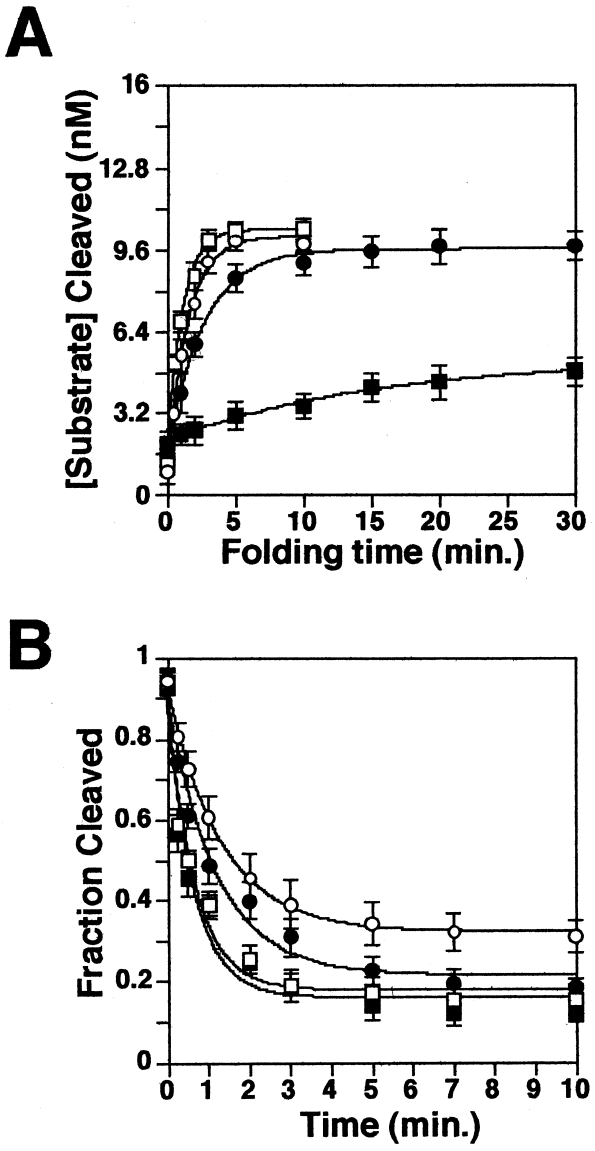

Fig. 2. Folding kinetics of A105G mutant ribozyme. A: Kinetics of active structure formation for the wild type and the A105G mutant at 37°C in the presence of 10 or 2 mM Mg^{2+}. Observed rates were 0.07 ± 0.00 min^{-1} for the wild type at 10 mM Mg^{2+} (filled square), 0.41 ± 0.02 min^{-1} for A105G at 10 mM Mg^{2+} (filled circle), 0.94 ± 0.04 min^{-1} for the wild type at 2 mM Mg^{2+} (open square), and 0.68 ± 0.04 min^{-1} for A105G at 2 mM Mg^{2+} (open circle). B: Kinetics of P3 helix formation in the wild type and the A105G mutant at 37°C in the presence of 10 or 2 mM Mg^{2+}. Observed rates were 1.6 ± 0.1 min^{-1} for the wild type at 10 mM Mg^{2+} (filled square), 0.84 ± 0.08 min^{-1} for A105G at 10 mM Mg^{2+} (filled circle), 1.5 ± 0.1 min^{-1} for the wild type at 2 mM Mg^{2+} (open square), and 0.77 ± 0.08 min^{-1} for A105G at 2 mM Mg^{2+} (open circle).

the concentration of magnesium ions (1.7-fold reduction by increasing Mg^{2+} ions from 2 to 10 mM, Fig. 2A, Table 1) in contrast with the more drastic effect on the $k_{overall}$ of the wild type (13-fold (this study) or 18-fold [12] reduction by increasing Mg^{2+} ion concentration from 2 to 10 mM, Fig. 2A, Table 1).

The rates of P3–P7 folding for the wild type and A105G mutant were also determined by the kinetic oligonucleotide hybridization assay technique (Fig. 2B). The k_{P3-P7} of the mutant was found to be 0.77 ± 0.08 or 0.84 ± 0.08 min^{-1} at 2 or 10 mM Mg^{2+}, respectively, whereas that of the wild type was 1.5 ± 0.1 or 1.6 ± 0.1 min^{-1} at 2 or 10 mM Mg^{2+}, respectively (Table 1). The rates for the mutant were therefore 1.9-fold slower than those for the wild type. However, the folding of the P3–P7 domain of both the mutant and the wild type was, similarly, essentially independent from the Mg^{2+} concentration (Fig. 2B, [12]).

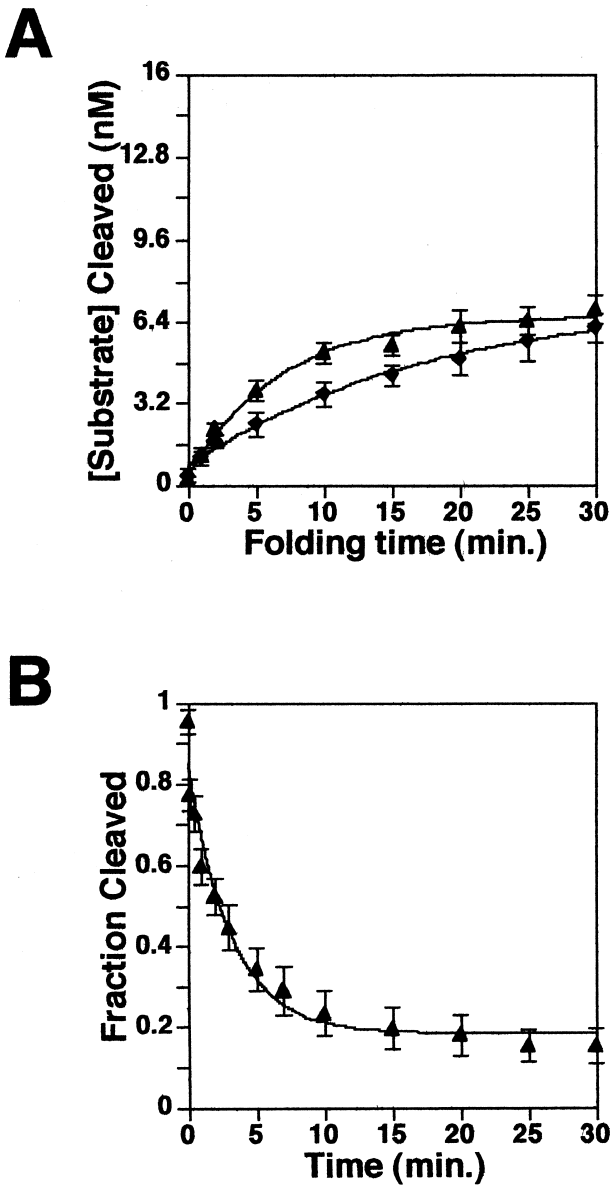

Fig. 3. Folding kinetics of C260G and A105G/C260G mutant. A: Kinetics of active structure formation for the C260G and the A105G/C260G mutants at 37°C in the presence of 10 mM Mg^{2+}. Observed rates were 0.06 ± 0.00 min^{-1} for C260G (filled diamond), and 0.15 ± 0.01 min^{-1} for A105G/C260G double mutant (filled triangle). B: Kinetics of P3 helix formation in the A105G/C260G double mutant at 37°C in the presence of 10 mM Mg^{2+}. Observed rate was 0.32 ± 0.03 min^{-1}.

3.4. Comparison with other fast-folding mutants

The single base substitutions at positions A183 (A-rich bulge) and U273 (P3 region) in two variant ribozymes, A183U and U273A, respectively, have been known to accelerate formation of the active structures (Fig. 1B) [13,22]. In the presence of 10 mM Mg^{2+}, the P3–P7 folding in A183U is accelerated about five-fold and the formation of the active structure about 1.6-fold (compared with the wild type) [13,23]. Formation of the active structure of A183U, however, is distinctly slower than that of the A105G mutant which folds 5.5-fold faster than the wild type with no reduction in ribozyme activity (Fig. 2A). In the case of a U273A mutant, the rate of P3–P7 folding equals that of the P4–P6 folding, and its active structure is formed at least 10–15-fold faster than the wild type at 4 mM Mg^{2+} [23,24]. Although no misfolding occurs, this mutation results in reduction of the catalytic activity by about two-fold (compared with the wild type) presumably because the mutation alters Mg^{2+} coordination, docking of P1 substrate helix and/or binding of a guanosine cofactor [23]. In contrast, A105G mutant is as active as the wild type under optimal conditions (2 mM Mg^{2+}) (Fig. 2A). The A183U and U273A mutants thus accelerate the formation of the active structure by increasing the rate of the P3–P7 domain folding. In the A105G mutant, a modest decrease in the P3–P7 folding accelerates the formation of the active structure, suggesting that J3/4×P6 base triples play a specific role in the final folding step of the ribozyme (Fig. 2A,B).

3.5. Folding kinetics of mutants with a defect at J6/7×P4

We determined $k_{overall}$ at 10 mM Mg^{2+} for a C260G mutant with a defect at J6/7×P4 to be 0.06 ± 0.00 min^{-1}. This is 6.8-fold less than that for the A105G mutant (0.41 min^{-1}) in which J3/4×P6 is disrupted, but the $k_{overall}$ remains virtually identical to that for the wild type (Fig. 3A). This implies that the rate of formation of the active ribozyme is identical for both the mutant and wild type ribozymes. (Note: we independently re-determined the value of $k_{overall}$ for the C260G mutant because the $k_{overall}$ for the wild type ribozyme was corrected recently from 0.61 min^{-1} [9] to 0.06 min^{-1} [12])

To examine the effects of double mutations at positions A105 and C260, $k_{overall}$ at 10 mM Mg^{2+} was determined for A105G/C260G mutant containing disruptions in both J3/4×P6 and J6/7×P4. The value for this mutant (0.15 ± 0.01 min^{-1}) was 2.3-fold higher than that of the wild type or C260G mutant although it is 2.7-fold less than that of the A105G mutant (compare Fig. 3A to Fig. 2A), suggesting that the A105G mutation is able to accelerate the formation of active ribozyme even in the presence of the disrupted J6/7×P4.

In a gain of activity assay, the reaction product was observed at the zero time point of the wild type or A105G ribozyme at 10 mM Mg^{2+} as shown in Fig. 2A. The burst represents the fraction of the ribozyme that folds within 30 s as described by Rook et al. [13]. This suggests the existence of a fast-folding pathway without kinetic traps which has recently been indicated by a single molecular analysis of the *Tetrahymena* ribozyme [22,25–27]. However, no fast-folding

fraction was detected for the C260G mutant (Fig. 3A). Although the nature of the fast-folding pathway is unclear, our results suggest that formation of J6/7×P4 base triples is essential for this folding pathway whereas J3/4×P6 base triples appear not to be involved as the fast-folding fraction is still observed in the A105G mutant (Fig. 2A).

The rate of P3–P7 folding was determined for the A105G/C260G double mutant (Fig. 3B). In the presence of 2 mM Mg^{2+}, the P3 region was cleaved completely by RNase H depending on the oligonucleotide complementary to P3 (data not shown), indicating the inability of the P3–P7 region to fold stably at 2 mM Mg^{2+}. The result is consistent with the observations that the double mutant is catalytically inactive (data not shown) and P3–P7 of the C260G mutant does not fold stably in the presence of 2 mM Mg^{2+} [10].

At 10 mM Mg^{2+}, the P3–P7 domain of the double mutant folds stably and its rate of kinetic folding is 0.32 ± 0.03 min^{-1} which is 5- or 2.6-fold lower than that of the wild type or A105G mutant, respectively (Fig. 3B). The P3–P7 domain of the C260G mutant is known to fold five-fold slower than the wild type ribozyme [10], indicating that the reduced P3–P7 folding rate for the double mutant is mainly due to the C260G mutation.

3.6. The base triples in kinetic folding

Analysis of the kinetic folding of a C260G mutant (with a defect at J6/7×P4 triples) at 10 mM Mg^{2+} by Zarrinkar and Williamson has shown that the C260G mutation slows formation of the P3–P7 domain by 4.8-fold compared with the wild type (Table 1, [10]), suggesting that formation of the triple-helical scaffold leads the folding of the P3–P7 domain [10]. In the present study, we show that a A105G mutation (disrupting J3/4×P6) also modestly slows the P3–P7 folding (1.9-fold). The fact that both A105G and C260G mutations cause inhibitive effects on P3–P7 folding suggests that both J3/4×P6 and J6/7×P4 triples are involved in guiding the folding of P3–P7 domain. At this step, J6/7×P4 triples seem to play a major role because the C260G mutation more severely retards P3–P7 folding (4.8-fold) than the A105G mutation (1.9-fold).

The rearrangement from I_F to the active ribozyme is the slowest step in the kinetic folding of the wild type ribozyme at 10 mM Mg^{2+} (Figs. 1 and 2). A mutation at A105G accelerates this step by 5.9-fold (Fig. 2A, Table 1) but the C260G mutation has no effect on this step (Fig. 3A, Table 1). This result indicates that the A105G mutation affects at least two steps in the kinetic folding: it slows folding of the P3–P7 domain but accelerates the formation of active ribozyme.

The acceleration in the formation of active ribozyme suggests that disruption or destabilization of J3/4×P6 triples significantly contributes to the fast rearrangement from I_F to the active ribozyme. This effect is likely to be totally or mostly independent from that of the J6/7×P4 triples because formation of the active structure of the A105G/C260G mutant occurs 2.1-fold faster than in the wild type while the C260G single mutation has no effect on this step (Fig. 3). These results indicate that the two base triples, J3/4×P6 and J6/7×P4, play distinct roles in the folding mechanism. J6/7×P4 mainly contributes to the induction of P3–P7 folding and J3/4×P6 to regulation of the rearrangement from I_F to the active ribozyme.

Recent analyses have indicated that transient tertiary interactions are required for structural rearrangement in the self-splicing of group I and II intron RNAs [28–30]. We have shown that the disruption of one set of base triples, J3/4×P6, connecting the two core domains, P4–P6 and P3–P7, enhances structural rearrangement for formation of the active structure of the *Tetrahymena* group I ribozyme in the presence of 10 mM Mg^{2+}. This prompted us to propose the following hypothesis. At lower concentrations of Mg^{2+}, the base triples are unstable so that fast and smooth rearrangement from I_F to the active structure is allowed to proceed without hindrance [11,12]. However, at higher concentrations of Mg^{2+}, they become more inflexible and this critical conformational rearrangement becomes the rate limiting step for building the active structure [11,12]. This hypothesis might explain why an A105G mutation that possibly relaxes the base triples is highly effective for rapid formation of the active structure in the presence of 10 mM Mg^{2+}. It also suggests that conformational rearrangement of the base triples in the wild type ribozyme might occur in the formation of the active structure under physiological conditions.

Acknowledgements: We thank Dr. Ruth Yu and members of the Inoue Laboratory for critical reading of the manuscript. This work was supported by Grants-in-Aid for Scientific Research on Priority Areas from the Ministry of Education, Science, Sports and Culture, Japan.

References

[1] Sclavi, B., Woodson, S.A., Sullivan, M., Chance, M.R. and Brenowitz, M. (1997) J. Mol. Biol. 266, 144–159.
[2] Sclavi, B., Sullivan, M., Chance, M.R., Brenowitz, M. and Woodson, S.A. (1998) Science 279, 1940–1943.
[3] Treiber, D.K. and Williamson, J.R. (1999) Curr. Opin. Struct. Biol. 9, 339–345.
[4] Chaulk, S.G. and MacMillan, A.M. (2000) Biochemistry 39, 2–8.
[5] Michel, F. and Westhof, E. (1990) J. Mol. Biol. 216, 585–610.
[6] Cech, T.R., Damberger, S.H. and Gutell, R.H. (1994) Nat. Struct. Biol. 1, 273–280.
[7] Golden, B.L., Gooding, A.R., Podell, E.R. and Cech, T.R. (1998) Science 282, 259–264.
[8] Brion, P. and Westhof, E. (1997) Annu. Rev. Biophys. Biomol. Struct. 26, 113–137.
[9] Zarrinkar, P.P. and Williamson, J.R. (1994) Science 265, 918–924.
[10] Zarrinkar, P.P. and Williamson, J.R. (1996) Nat. Struct. Biol. 3, 432–438.
[11] Pan, J., Thirumalai, D. and Woodson, S.A. (1999) Proc. Natl. Acad. Sci. USA 96, 6149–9154.
[12] Rook, M.S., Treiber, D.K. and Williamson, J.R. (1999) Proc. Natl. Acad. Sci. USA 96, 12471–12476.
[13] Rook, M.S., Treiber, D.K. and Williamson, J.R. (1998) J. Mol. Biol. 281, 609–620.
[14] Ikawa, Y., Shiraishi, H. and Inoue, T. (2000) Nat. Struct. Biol. 7, 1032–1035.
[15] Williamson, C.L., Desai, N.M. and Burke, J.M. (1989) Nucleic Acids Res. 17, 675–689.
[16] Imai, Y., Matsushima, Y., Sugimura, T. and Terada, M. (1991) Nucleic Acids Res. 19, 2785.
[17] Milligan, J.F., Groebe, D.R., Witherell, G.W. and Uhlenbeck, O.C. (1987) Nucleic Acids Res. 15, 8783–8798.
[18] Zarrinkar, P.P. and Williamson, J.R. (1996) Nucleic Acids Res. 24, 854–858.
[19] Treiber, D.K. and Williamson, J.R. (2000) Methods Enzymol. 317, 330–353.
[20] Chastain, M. and Tinoco Jr., I. (1992) Biochemistry 31, 12733–12741.
[21] Michel, F., Ellington, A.D., Couture, S. and Szostak, J.W. (1990) Nature 347, 578–580.
[22] Pan, J., Deras, M.L. and Woodson, S.A. (2000) J. Mol. Biol. 296, 133–144.

[23] Treiber, D.K., Rook, M.S., Zarrinkar, P.P. and Williamson, J.R. (1998) Science 279, 1943–1946.
[24] Pan, J. and Woodson, S.A. (1998) J. Mol. Biol. 280, 597–609.
[25] Pan, J., Thirumalai, D. and Woodson, S.A. (1997) J. Mol. Biol. 273, 7–13.
[26] Russell, R. and Herschlag, D. (1999) J. Mol. Biol. 291, 1155–1167.
[27] Zhuang, X., Bartley, L.E., Babcock, H.P., Russell, R., Herschlag, D. and Chu, S. (2000) Science 288, 2048–2051.
[28] Chanfreau, G. and Jacquier, A. (1996) EMBO J. 15, 3466–3476.
[29] Tanner, M.A., Anderson, E.M., Gutell, R.R. and Cech, T.R. (1997) RNA 3, 1037–1051.
[30] Tanner, M.A. and Cech, T.R. (1997) Science 275, 847–849.
[31] Lehnert, V., Jaeger, L., Michel, F. and Westhof, E. (1996) Chem. Biol. 3, 993–1009.
[32] Treiber, D.K. and Williamson, J.R. (2001) J. Mol. Biol. 305, 11–21.